A complementary energy approach accommodates scale differences in soft tissues

Pablo Saez[a,b], Steven J. Eppell[c], Roberto Ballarini[d], F. Rodriguez Matas[e]

[a] *Laboratori de Càlcul Numèric (LaCàN), Universitat Politècnica de Catalunya-BarcelonaTech.*
[b] *Barcelona Graduate School of Mathematics–BGSMath, Barcelona, Spain*
[c] *Department of Biomedical Engineering, Case Western University, Cleveland, OH 44106, United States.*
[d] *Department of Civil and Environmental Engineering, University of Houston, Houston, TX 77204, United States.*
[e] *Dipartimento di Chimica, Materiali e Ingegneria Chimica "Giulio Natta", Politecnico di Milano, Milan, Italy.*

Abstract

The mechanics of biological entities, from single molecules to the whole organ, has been extensively analyzed during the last decades. At the smaller scales, statistical mechanics has fostered successful physical models of proteins and molecules, which have been later incorporated within constitutive models of rubber-like materials and biological tissues. At the macroscopic scale, the additive decomposition of energy functions i.e., a parallel arrangement of the tissue constituent, has been recurrently used to account for the internal heterogeneity of soft biological materials. However, it has not yet been possible to unite the mechanics at the tissue level with the actual response of the tissue components. Here, we exemplify our approach using cardiovascular tissue where the mechanical response at the tissue scale is in the range of kPa whereas the elastic modulus of collagen, the main component of the vascular tissue, is in the range of MPa GPa. In this work we develop a novel theoretical framework based on a complementary strain energy function that builds-up on a full network model. The complementary strain energy function introduces naturally an additive decomposition of the deformation gradient for the tissue constituents, i.e an arrangement in series of the constituents. We demonstrate that the macroscopic response of the tissue can be reproduced by just introducing the underlying mechanical and structural features of the micro-constituents, improving in a fundamental manner previous attempts in the mechanical characterization of soft biological tissues. The proposed theoretical framework unveils a new direction in the mechanical modeling of soft tissues and biological networks.

Keywords: Soft Biological Tissues, non-affine deformations, micro-sphere.

1. Introduction

The influence of mechanics in biology spans from single proteins through cells and tissues to entire organs [29, 44, 31], so physicists, mathematicians, and engineers have focused on its characterization for several decades. For example, the mechanics of adhesion molecules [56] determine the dynamics of cell adhesion [19, 24, 17] and, therefore, of cell motility. The mechanics of actin have fundamental implications in a large number processes in mechanobiology such as cytokinesis and ring contraction [6, 51] and cancer progression [11]. Organization of the extracellular-matrix (ECM) at the tissue and organ level dictates the

mechanics of the tissue in health and diseases such as aneurysm formation [50]. Understanding how all these constituents arrange in biological networks is key to both understanding their mechanical response and also for the design of biomedical materials [26, 34] and tissue engineering [25, 33].

Today, most of the mechanical models for soft tissues come from the early developments in rubber elasticity [20]. The theory of non-linear hyperelasticity has been the starting point from which phenomenological continuum models for anisotropic soft biological tissues have been developed at the macroscale. On the contrary, the concepts of Gaussian and non-Gaussian statistical mechanics have been used at the microscale. The Freely Joined Chain or the Worm-like chain have described successfully the mechanics of DNA molecules [10] and collagen molecules [9]. The introduction of suitable averaging methods allowed to obtain the macroscopic constitutive law of networks, such as actin filaments [35, 8, 32]. In this regard, different continuum models based on single filament statistical mechanics have been also proposed [2, 38, 42, 1] to describe the mechanical behavior of tissues with outstanding accuracy.However, despite using an accurate description of the microstructure, a significant mismatch in the mechanical properties of the constituents at the microscale is observed.

A clear example of multi-scale modeling in biological networks appears in cardiovascular tissue which is among the most studied biological entities in mechanics. Arterial wall, the specific system we focus on in this work to exemplify our theoretical derivation, is a highly heterogeneous material with a complex architecture made up of collagen and elastin (see Fig. 1). In this regard, most models for arterial mechanics rely on the mechanical contribution of these two components. The stiffness of the cardiovascular tissue (Fig. 1a) has been reported in the range of kPa (see [16, 22, 28, 45] among many others) whereas the mechanical stiffness of the micro-constituents at the fiber and fibril scale e.g., collagen, (Fig. 1b) are found to be orders of magnitude higher, in the range of MPa GPa [18, 52, 53]. To date, no mechanical model has been able to reconcile the differences between the mechanical properties measured at the microscale with those obtained at the tissue level.

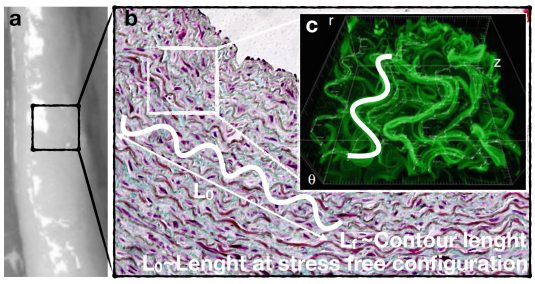

Figure 1: Sample of a carotid artery taken from pig (a). Histological study of porcine carotid tissue by Masson's trichrome stain when clear pink color is elastin, red is muscle, and a blue/green is the collagen fibers (b). 3D reconstruction of the entanglement of collagen bundles in the arterial tissue (adapted from [48]) (c). The white line represents the waviness of the collagen bundles a length L_0 at the reference configuration and a contour length L_f.

2. Methods

2.1. Continuum modeling of soft tissues

To motivate our work, we start by describing the basic kinematics and the energy function, or Strain Energy Density Functions (SEDF) Ψ, required to derive a **macroscopic stress-strain relation** as $\mathbf{P} = \partial_{\mathbf{F}}\Psi$, with $\mathbf{P}$ the first Piola-Kirchhoff stress tensor, and $\mathbf{F}$ the deformation gradient [36]. The deformation gradient $\mathbf{F} = \nabla_X \varphi(\mathbf{X}, t) \ : T\Omega_0 \rightarrow T\Omega_t$, represents the linear tangent map from the tangent space $T\Omega_0$ to the time–dependent tangent space $T\Omega_t$, and $\mathbf{P}$ is the thermodynamic force conjugate to $\mathbf{F}$. In the classic approach, the SEDF is written in the form $\Psi_T = \sum_1^i \Psi^i$, with i the number of micro-constituents of the tissue e.g., collagen and elastin. The additive decomposition adopted for the SEDF inherently assumes that the different constituents work in parallel, meaning that the deformations are affine and that different stress values are obtained for each constituent. Many phenomenological models [39, 15, 27] have been used to define the mechanical behavior of biological tissues through different SEDFs. Other approaches make use of non-Gaussian and semi-flexible filament models to define network models, such as the early 3-chain and 8-chain models[2], or the non-affine micro-sphere model [38]. In this work, we have adopted a full network model [54, 55] which provides an elegant approach that has demonstrated excellent results with arterial tissue [1, 49].

Within the full-network model, we characterize the energy function of the components at the micro-scale, ψ, and the SEDF at the macro-scale $\Psi = \langle \psi(\lambda) \rangle$ through an homogenization of the quantities of interest $\langle \bullet \rangle$, the energy function in our case, over the unit sphere $\mathbb{U}^2$ as

$$4\,\pi \langle \psi(\lambda) \rangle \ = \ \int_{\mathbb{U}^2} \psi(\lambda)\, \mathrm{d}A. \tag{1}$$

The integral in Eq. 1 is performed numerically as the sum along a number of integration directions on the micro-sphere $\mathbf{r}_i$ and weights w_i such that $\int_{\mathbb{U}^2} (\bullet)\, \mathrm{d}A \approx \sum_{i=1}^{m} (\bullet)^i w_i$. From now on, we will use m=184 (see, e.g., [3, 1] for details). To reproduce the mechanical response of the tissue, we first obtain the stress measures deriving $\langle \psi_i(\lambda) \rangle$ with respect to the associated strain measure [36, 38]. Considering an additive decomposition of the SEDF as $\Psi = \Psi_c + \Psi_e$, representing the collagen and elastic components respectively. Hence, the macroscopic Kirchhoff stress can be written as

$$\boldsymbol{\tau} \ = \boldsymbol{\tau}_c + \boldsymbol{\tau}_e = \ \langle \left(\partial_\lambda \psi_c + \partial_\lambda \psi_e\right) \lambda^{-1}\, \mathbf{t} \otimes \mathbf{t} \rangle \tag{2}$$

where $\mathbf{t} \ = \ \mathbf{F} \cdot \mathbf{r}$, $\lambda_{\mathrm{i}} \ = \ \|\mathbf{F} \cdot \mathbf{r}^i\|$ are the stretches along $\mathbf{r}^i$, and ψ_c and ψ_e are the energy function for the collagen and elastin components respectively.

2.2. Continuum modeling of the micro-structure

Next, it remains to define the mechanical behavior of each constituent and its structural organization at the microscale in order to define the mechanical response at the macro-scale, i.e. the arterial tissue. First,

we define the **mechanics of single filaments**, which we identify with collagen and elastin fibrils. To define the SEDF for the different constituents, we start by defining the extension of the filament as a function of the force acting on it as

$$r = L - \frac{6\Delta L_0}{\pi^2}\sum_k \frac{1}{k^2+\phi}, \text{ where } \phi = \frac{6}{\pi^2}\frac{P\Delta L_0}{r_0 c_1}, \tag{3}$$

where P is the applied stress to the filament, L is the full length of the filament at $P \mapsto \infty$, $\Delta L_0 = L - r_0$ with r_0 the resting length of the filament for $P = 0$ i.e., the stress-free length, and c_1 a material parameter with units of stress identified from experiments.

This phenomenological extension-force relationship recalls the result of a semi-flexible network, widely used in actin networks [35, 43]. However, in this work, this is assumed as a phenomenological extension-force law only requiring $L > r_0$. Therefore, Eq. 3 must be seen as a suitable description of the stretch-force relation for the single filament within the continuum mechanics framework. Note that, other constitutive relationships can be adopted as long as they describe the mechanical system correctly.

A standard way of simplifying the series in Eq. 3 is by means of the Langevin function, $\mathcal{L} = coth(\chi) - 1/\chi$ with $\chi = \pi\sqrt{\phi}$ [43]. Inverting now the Langevin function we can obtain an expression for the force as a function of the stretch of the filament, $\lambda = r/r_0$. Integrating along the length as $\psi = \int P(\lambda)d\lambda$ we can derive a form for the energy function as [43]

$$\psi = c_1\left(\frac{3}{2}\frac{L - r_0}{L - r_0\lambda} - \log\frac{3r_0 - 2L - r_0\lambda}{3(L - r_0\lambda)(L - r_0)}\right) - \mathcal{D}, \tag{4}$$

where $\mathcal{D}$ is a constant equal to the initial strain energy density from the filaments. From Eq. 4 we can derive the Kirchhoff stress as $\tau = \partial_\lambda \Psi_c \lambda^{-1}$. We show in Fig. 2 the mechanical response of the proposed phenomenological model, which reproduce a zero stress for $\lambda = 1$ and an asymptotically increasing stress as r/L $\mapsto$ 1.

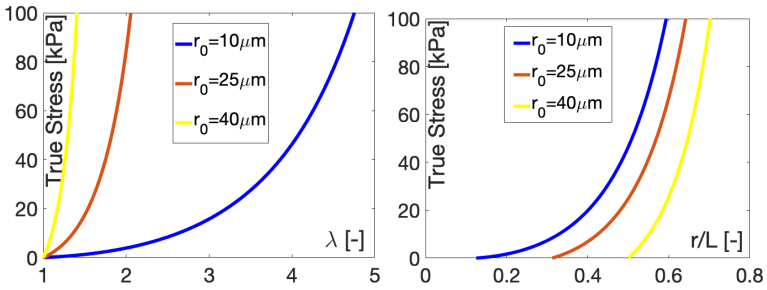

Figure 2: Stress response of the phenomenological model in Eq. 4 for L=80μm and a combination of different stress-free initial lengths. On the left, true stress as a function of the stretch of the fibril $\lambda = r/r_0$. On the right, true stress as a function of r/L.

2.3. Anisotropic description of the tissue

Once defined the mechanical behavior for the single filaments, we proceed to assemble them to describe the collagen network, considered the most determining component in terms of the mechanical response of the tissue. The main features of the collagen network that contribute toward the mechanics of the tissue are the anisotropic entanglement of the collagen fibers and its waviness, which can be obtained from additional experimental observations. *The anisotropic arrangement of the collagen structure* can be explicitly considered by means of an orientation distribution function (ODF) [49]. The Bingham ODF [5], $\rho(\mathbf{r}^i;\, \mathbf{Z},\, \mathbf{Q})$ has been recently proposed to describe experimental results from polarized light microscopy [49]. The Bingham distribution is defined as

$$\rho(\mathbf{r};\mathbf{Z},\mathbf{Q})\frac{dA}{4\pi} = [F_{000}(\mathbf{Z})]^{-1}\exp(\mathrm{tr}(\mathbf{Z}\cdot\mathbf{Q}^{\mathrm{T}}\cdot\mathbf{r}\cdot\mathbf{r}^{\mathrm{T}}\cdot\mathbf{Q}))\frac{dA}{4\pi}, \tag{5}$$

where $\mathbf{Q}\in\mathbb{Q}^3$, with $A=\mathbf{Q}\cdot\mathbf{Z}\cdot\mathbf{Q}^t$, determines the preferential orientation of the probability distribution in the surface of the unit sphere and, consequently, in the arterial wall. $\mathbf{Z}$ is a diagonal matrix with eigenvalues $\kappa_{1,2,3}$ that can be interpreted as concentration parameters along the three orthogonal directions in space, i.e. along the circumferential, radial and axial vessel wall directions, respectively. The difference between pairs of eigenvalues, i.e. $\Delta\kappa_{1,2,3}=[\kappa_1-\kappa_2,\kappa_1-\kappa_3,\kappa_2-\kappa_3]$ determines the shape of the distribution. Therefore, one of the $\Delta\kappa_{1,2,3}$ may be set to zero without reducing the versatility of the distribution. With two eigenvalues $\Delta\kappa_{1,2,3}$ equal to zero, the von Mises ODF is recovered. Finally, the factor

$$F_{000}(\mathbf{Z}) = \frac{1}{4\pi}\int_{\mathbb{U}^2}\exp(\mathrm{tr}(\mathbf{Z}\cdot\mathbf{r}\cdot\mathbf{r}^{\mathrm{T}}))dA. \tag{6}$$

is introduced so that $1/(4\pi)\int\rho dA=1$.

The inset in Fig. 4 shows an example of the Bingham ODF for the distal location of a carotid artery. The SEDF for the tissue reads now as $\langle\rho\psi_i(\lambda)\rangle$.

2.4. Waviness description of the assembled filaments

We introduce the *waviness of assembled collagen fibrils* [48] (see inset in Fig. 1), that are observed in most soft tissues and has been proposed to play an important role in the tissue response. Note that this waviness differs from the undulation of the filament mechanics in Eq. 4 in that the waviness represents a macroscopic structural feature that describes the actual rippling of the collagen fibers within the tissue. Waviness has been usually described using a Gaussian distribution [57, 12]. In this work, however, we choose to describe the crimp of collagen fibers through a Beta probability density function for which the random variable is limited to a finite interval

$$f_L(\mathcal{P}_s;\alpha,\beta) = \frac{\Gamma(\alpha+\beta)}{\Gamma(\alpha)\Gamma(\beta)}\,\mathcal{P}^{\alpha-1}(1-\mathcal{P})^{\beta-1}, \tag{7}$$

where $\Gamma(\bullet)$ represents the Gamma function and the shape parameters are $\alpha=4.47$ and $\beta=1.76$ [48]. As the tissue deforms, the collagen fibrils align with the stretching direction reducing the waving of the fibers. We include $\mathcal{P}_s\in(0,1)$, as defined in [48], as a measure of the waviness of the fiber. $\mathcal{P}_s=1$ indicates a

totally straight fibril bundle and as we lower its value we obtain a more crimped fiber. We take the same parameter $\mathcal{P}_s$ as a measure of the deformation required for a straight bundle to start to stretch. Once a bundle is completely straight, the mechanical behavior of individual collagen fibrils, Ψ, takes over. Therefore, we compose the stretch of a single bundle as the deformation required to unfolded it up to $\mathcal{P}_s = 1$ and the deformation from the fully extended configuration of the bundle, $\lambda_T = \lambda \cdot \mathcal{P}_s$. Finally, we integrate the waviness of the collagen network with the mechanical behavior of the fibrils bundle, its anisotropy and spatial distribution through the averaged SEDF in Eq. 1 to obtain

$$\Psi_c = \int_{\mathbb{U}^2} \int_0^1 f_L(\mathcal{P}_s; \alpha, \beta) \rho(\mathbf{r}^i;\, \mathbf{Z},\, \mathbf{Q})\, \psi(\lambda, \mathcal{P}_s) \mathrm{d}\mathcal{P}_s \mathrm{d}A. \tag{8}$$

2.5. A complementary strain energy function full-network model

To generalize this idea within a consistent thermodynamic formulation, we take advantage of the complementary energy density function (cSEF) (see [41, 47] among others). Recalling the definition of the deformation gradient $\mathbf{F}$, we use the polar decomposition to write $\mathbf{F} = \mathbf{R} \cdot \mathbf{U}$, where $\mathbf{U}$ is the symmetric positive definite right stretch tensor, defined with respect to the reference configuration. The unique $\mathbf{R}$ is a proper orthogonal tensor, with $\det(\mathbf{R}) = 1$, called the rotation tensor. Following [41], a symmetric stress tensor $\boldsymbol{\tau}_J$, which states for a symmetrized Biot or Jauman stress tensor, is defined as

$$2\boldsymbol{\tau}_J = \mathbf{P}\mathbf{R} + \mathbf{R}^T\mathbf{P}^T. \tag{9}$$

such that $\mathbf{P} : \dot{\mathbf{F}} = \boldsymbol{\tau}_J : \dot{\mathbf{U}}$. $\boldsymbol{\tau}_J$ can be seen as a co-rotated material stress tensor. This definition of the stress and strain conjugates have large implications in the constitutive modelling of hyperelastic materials such that a constitutive law can be written as a function $\mathbf{P}(\mathbf{F})$. The law must fulfill the frame indifferent conditions. However, $\boldsymbol{\tau}(\mathbf{U})$ is already frame indifferent. In consequence we can also write

$$2\boldsymbol{\tau}(\mathbf{U}) = \mathbf{P}(\mathbf{U}) + \mathbf{P}^T(\mathbf{U}). \tag{10}$$

Under the assumption of a SEDF per unit of volume in the deformed configration Ψ we can define $\mathbf{P} = \partial_{\mathbf{F}}\Psi$ and $\boldsymbol{\tau}_J = \partial_{\mathbf{U}}\Psi$. In view of these definitions, and given the equality $\mathbf{P} : \mathbf{F} = \boldsymbol{\tau}_J : \mathbf{U}$ we can define now a complementary SEDF per unit volume $\hat{\Psi}$ such that

$$\Psi + \hat{\Psi} = \mathbf{P} : \mathbf{F} = \boldsymbol{\tau}_J : \mathbf{U}, \tag{11}$$

where $\hat{\Psi}$ is a function of $\mathbf{P}$ or $\boldsymbol{\tau}_J$. It can be shown that $\hat{\Psi}$ takes the same values whatever variables are chosen for the definition and, therefore, possesses frame indifference inherently. Under local invertibility of $\boldsymbol{\tau}_J(\mathbf{U})$ we can define $\mathbf{U} = \partial_{\boldsymbol{\tau}_J}\hat{\Psi}$ and $\mathbf{F} = \partial_{\mathbf{P}}\hat{\Psi}$.

Within our full-network model, the cSEDF for a single filament can be defined in a one-dimensional energetic frameworks as

$$\psi + \hat{\psi} = \mathrm{P}\lambda, \tag{12}$$

where we have use the First Piola-Kirchhoff stress tensor projection $\mathrm{P} = \mathbf{P} : [\mathbf{r} \otimes \mathbf{t}]$.

In order to define $\hat{\psi}$ we can make use of the Legendre transformation in Eq. 12, given an expression of the energy function. Therefore, the methodology is applicable to any existing energy function. In our particular case, however, the expression for $\hat{\psi}$ for a single filament was dereived by integrating the stretch, $\lambda = r/r_0$, obtained from Eq. 3 along the stress, P, i.e., $\hat{\psi} = \int \lambda(\mathrm{P})\ \mathrm{dP}$

$$\hat{\psi} = c_1 \left[\frac{1}{6} \frac{\pi^2 L}{L - r_0} \phi - \sum_k \log\left(\frac{k^2 + \phi}{k^2} \right) \right], \tag{13}$$

where c_2 is a material parameter with units of stress, and ϕ is as defined in Eq. 3.

The total complementary SEDF, weighted by its percent amount of collagen and elastin, Ξ_c and Ξ_e, is given as

$$\hat{\Psi}_T = \hat{\Psi}_c + \hat{\Psi}_e = \Xi_c \langle\, f_L\, \rho\, \hat{\psi}_c \rangle + \Xi_e \langle\, \hat{\psi}_e \rangle, \tag{14}$$

where the averaged complementary energy function in the full-network model for the collagen and elastin network results

$$\hat{\Psi}_c = \Xi_c \int_{\mathbb{U}^2} \int_0^1 f_L(\mathcal{P}_s; \alpha, \beta) \rho(\mathbf{r}^i;\, \mathbf{Z},\, \mathbf{Q})\, \hat{\psi}_{\mathrm{c}}(\mathrm{P}) \mathrm{d}\mathcal{P}_s \mathrm{d}A \qquad \text{and} \qquad \hat{\Psi}_e = \Xi_e \int_{\mathbb{U}^2} \hat{\psi}_{\mathrm{e}}(\mathrm{P}) \mathrm{d}A. \tag{15}$$

Here, the values for the collagen and elastin fractions are $\Xi_c = 65\%$ and $\Xi_e = 35\%$, respectively, following experimental observations [40]. We will keep these values fixed in what follows. After deriving with respect to the conjugate stress measure $\mathbf{P}$ we obtain the total as well as the collagen and elastin deformation gradient:

$$\mathbf{F}_T = \partial_{\mathbf{P}} \hat{\Psi}_c + \partial_{\mathbf{P}} \hat{\Psi}_e = \Xi_c \mathbf{F}_c + \Xi_e \mathbf{F}_e \tag{16}$$

We make use of the chain rule in $\partial_{\mathbf{P}} \hat{\psi} = \partial_\phi \hat{\psi} \partial_{\mathbf{P}} \phi$ to define

$$\partial_{\mathbf{P}} \hat{\psi} = \frac{6(L - r_0)}{\pi^2 r_0} \left[\frac{\pi^2 L}{6(L - r_0)} - \sum_k \frac{1}{k^2 + \phi} \right] \mathbf{r} \otimes \mathbf{t} = \lambda \mathbf{r} \otimes \mathbf{t}. \tag{17}$$

The deformation gradients for the collagen and elastin phase can be described as

$$\mathbf{F}_c = \langle f_L\, \rho\, \lambda_c\, \mathbf{r} \otimes \mathbf{t} \rangle \text{ and } \mathbf{F}_e = \langle \lambda_e\, \mathbf{r} \otimes \mathbf{t} \rangle. \tag{18}$$

The additive decomposition of the complementary SEDF naturally impose an additive decomposition of the deformation gradient into the collagen and elastin deformation gradient. Therefore, the non-affinity of the model is controlled by the mechanical and structural parameters of each component of the network: the amount of constituents, the waviness, the anisotropy and the stretch of each direction. For a discussion on

the addition of a volumetric term for the incompressibility constraint within the complementary SEDF, see [47].

3. Results

The presented framework has been applied to describe the mechanical behavior of arterial tissue. We first characterize the behavior of isolated collagen fibrils using Eq. 3. We then proceed to describe the mechanical behavior of arterial tissue (carotid) using the classical SEDF approach and the proposed complementary SEDF approach.

3.1. Mechanical response of collagen fibrils

We use the energy function in Eq. 4 to describe the mechanical response of an isolated collagen fibrils. Collagen fibrils have a distinctive architecture resulting from their self-assembly from soluble single molecules [21]. The entropically driven formation of micro-fibrils is initiated by cleavage of the terminal C-propeptides of the procollagen molecule. This results in both lateral and axial molecular association forming fibrils (10-200 nm in diameter) with a distinctive axial periodic pattern of 67 nm due to precise parallel molecular overlap likely driven by electrostatic interactions. A number of covalent crosslinks, e.g lysyl oxidase enzymatic links and glucose derived glucosepane links), stabilize the fibril assembly providing integrity and strength. At length scales greater than the single fibril diameter, bundles of collagen fibrils interwoven with layers of non-collagenous glycoproteins form. While it is known that there are significant helical structures spanning the sub-molecular up through the microscale fibril bundle level [46], we have not included this detail in our model. We fit a tensile test of isolated collagen fibrils (see [52] for details of the experimental procedure and results) in a fully straight reference configuration by means of a least-square method using τ. Results are plotted in Fig. 3. We obtain a value of L=13.46μm and r_0=3.54μm and $c_1 = 410.43kPa$ with a normalised root mean square error (NRMSE) of 0.012. This result shows that the phenomenological extension-force relationship described in Eq. 3 accurately describes the mechanics of collagen fibrils.

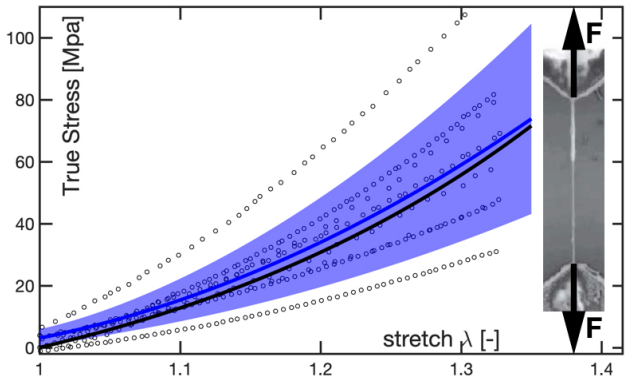

Figure 3: Circles shows the mechanical response of 9 data set of isolated collagen fibril. Blue solid line is the mean of all data set and blue shadow represents the standard deviation. Black solid line is the solution of the model described in Eq. 4 with values $L = 13.46$ μm and $r_0 = 3.54\mu$m and $c_1 = 410.43$ kPa.

3.2. Mechanical response of arterial tissue through a SEDF

We aim at modeling the mechanical behaviour of arterial tissue by making use of the SEDF in Eq. 1, which represents a non-linear full-network model. The elastin network is modeled using a one-dimensional Neo-Hookean law with $\psi_e = 2\mu(\lambda^2 - 1/\lambda)$ in each orientation direction, whereas collagen is modelled using Eq. 15 with $\mathcal{P}_s = 1$ i.e., no waviness is considered. Hence, the parameters to be identified result: L, r_0 and c_1 for the collagen network, and μ for the elastin network. The parameters of the Bingham distribution have been taken from [49] resulting in the distribution shown in the inset of Fig. 4. The material parameters for the constitutive models were obtained by means of a nonlinear regression analysis of uniaxial test data of pig carotid artery reported in [23]. The resulting material parameters were L=5.81μm, r_0=3.26μm and c_1= 42.67 kPa for the collagen network, and μ=40.1 kPa for elastin. As shown in Fig. 4, this approach is able to fit the experimental data satisfactorily with a normalized root mean square error (NRMSE) of 0.045. However, the stress-like parameter of the collagen network, c_1, is an order of magnitude lower than the one identified in the previous section on single collagen fibrils i.e., 42.67 kPa vs 410.43 kPa. For completeness, we also fit the model considering the waviness of the collagen fibers i.e. $\mathcal{P}_s \in [0, 1]$ described in Section 2.4 to see if this helped to improve these discrepancies. Unfortunately, incorporating the waviness did not improve the results.

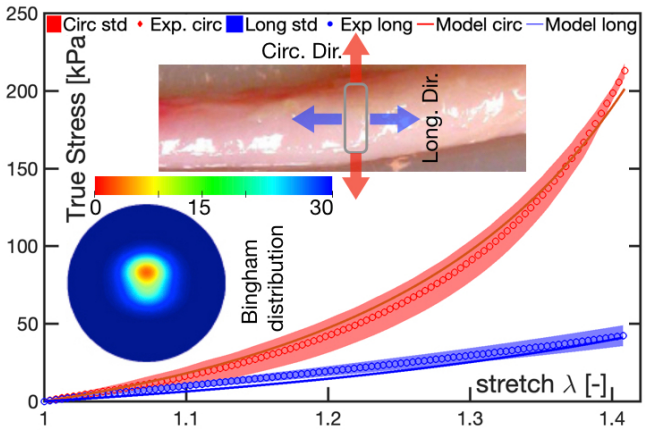

Figure 4: Stress-strain relation obtained from experimental test is fitted, by means of a least-square procedure, to obtain the material parameters that better describe the mechanical behavior. The elastin network is the only component that mechanically entangles in the longitudinal direction (blue) since the collagen is preferentially aligned in the circumferential direction. In the circumferential direction (red), the main contribution to the mechanics of the tissue is the collagen fibril bundles. Discrete marks represent the mean of 13 experimental data and shadows show the standard deviation. Lines represent the model results. Inset on top shows the sketch of the circumferential and longitudinal directions of the artery, in which the artery is cut and uniaxial tests are performed. Inset on the bottom shows the resulting Bingham distribution taken from [49], with two families of fibers and $\Delta\kappa^{f1}_{1,2,3} = [13.5, 0.0, 25.2]$ and $\Delta\kappa^{f2}_{1,2,3} = [14.7, 0.0, 26.6]$.

3.3. Mechanical response of arterial tissue through a complementary SEDF

The discrepancies in the material parameter between the micro- and macro-scales found in the previous sections give the key motivation of this work, namely: *The mechanical behavior of the micro-structural*

collagen fibrils do not resemble the mechanical response of the tissue at the macroscopic scale. In other words, the material parameters of the collagen network identified using the SEDF approach are of little physical meaning. Further, if for the collagen network SEDF model in Section 3.2 we use the material parameters identified in Section 3.1 (at the microscale), and reproduce the same uniaxial protocol described in [23] the results is in an over stiff response of the tissue (see black solid line in Fig. 5). Since the anisotropy and the waviness of the collagen network can be determine by direct experimental observations, the discrepancies in the mechanical response between the tissue scale and the single fibril scale can only arise from the definition of the energy functions. In this particular, we wonder if the previous modeling limitations arise from the assumption associated with the SEDF approach that elastin and collagen work in parallel. In this case, for a given stretch, the collagen (much stiffer than elastin) dominates the mechanical response of the tissue. On the contrary, if a series arrangement is assumed for the constituents, the transmitted force is the same for all constituents whereas the varying quantity is the displacement of each element that occurs in a non-affine manner i.e., $u_T = \sum_1^i u_i$, where u_i is the displacement of each constituent. In this regard, analysis of the tissue strains through confocal microscopy have shown that the individual tissue components deform in a non-affine manner [4, 14, 30] during the reorganization and damage of the sclera's collagen fiber arrangement under loading [13] and [37]. Consequently, we asked ourselves if a series construct is able to reproduce the mechanical response of cardiovascular soft tissues at the macroscale while incorporating the actual mechanical properties of the constituents determined at the microscale. In an effort to give an answer to this question, we have developed the complementary SEDF described in Section 2.5.

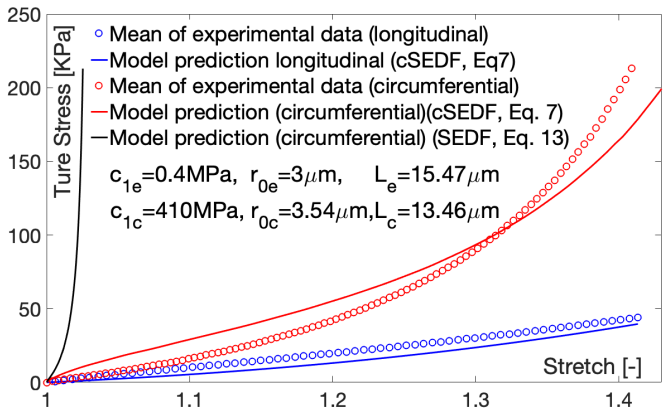

Figure 5: Experimental data and model results for the complementary full-network model. Red and blue lines shows the results of the cSEDF when the mechanical response of the fibrils are included in the full-network model. Black line shows the network response when the SEDF is used to describe the tissue.

We incorporated in the complementary SEDF model described in Section 2.5, the properties of the collagen fibrils identified in Section 3.1. For the elastin we use the same constitutive law, described in Eq. 13. We first fit the longitudinal direction in which only elastin is present. Then, we included the resulting values (see Figure 5) to reproduce the mechanical test at both the circumferential and longitudinal directions. The parameters associated with the anisotropy and waviness have been left unaltered with respect to Section 3.2.

It is important to recall that we do not perform any further fitting procedure of the mechanical parameters at the tissue scale. In other words, at the tissue scale we have just assembled the contributions from the different constituents. Figure 5 shows that the cSEDF is able to reproduce the mechanical response of the tissue with a NRMSE=0.175. Clearly, the cSEDF is able to unite the mechanical response of the micro- and macro-scale of the tissue.

4. Conclusions

In short, we have introduced a new reasoning in the mechanical modeling of soft biological tissue, in which the complex architecture of the network components works concomitantly in series and not in parallel, as usually assumed. Here, we evaluate the behavior of the complementary SEDF against a standard SEDF within the same full-network model. Further comparison between different chain models, full-network models and full-network versus invariant and stretch-based models can be found elsewhere, e.g. in [38, 7, 42], among others. Through the definition of complementary energies, we have formalized in a thermodynamically consistent manner a full-network model where a description of the mechanics of the tissue components has been introduced. We have made use of the main structural features of the collagen network, i.e. the orientation, distribution and waviness of the collagen network and the mechanical properties of the elastin and collagen fibrils, to define ad-hoc the mechanical response of the tissue. The structural aspects of the network were recovered from experimental data, and a Bingham distribution function [49] and the Beta probability function [48] were used to define the orientation and waviness of the collagen fibrils respectively. The mechanical properties of collagen fibrils were obtained independently from experimental data at the micro-scales. The mechanical properties of elastin were computed at the low strain regime of the tissue, in which only elastin bears the mechanical load. Future experimental data on individual tissue components in this and other tissues could be introduced directly in our theoretical approach. Both the mechanical and structural information were introduced ad-hoc in the complementary strain energy function, in which an additive decomposition of the deformation gradient appeared naturally. Therefore, we have been able to unite the mechanics of the collagen and elastin with the mechanical behavior at the artery without any further fitting at the tissue scale which represents a fundamental step forward in the modeling of soft biological tissues. Our present contribution, however, relies on the stresses as the primary field variables, whereas the deformation is obtained as a work conjugate from the complimentary energy function. Therefore, we cannot evaluate stresses from a displacement-driven experiment in complex loading scenarios. This approach may be cumbersome when implementing it within the finite element method. Therefore, we believe that this contribution can be the initial seed for an interesting discussion and research on the mechanical description of biological tissues in the future. In conclusion, we believe that such simple physical reasoning is the answer to realistically integrating the information at the different scales of biological tissues and molecules and to open a novel approach in the modeling of soft biological tissue, and polymer networks in general.

Acknowledgements

P.S acknowledges the support of the Generalitat de Catalunya 2017-SGR-1278.

References

[1] Alastrué, V., Martinez, M.A., Doblare, M., Menzel, A., 2009. Anisotropic micro-sphere-based finite elasticity applied to blood vessel modelling. J. Mech. Phys. Solids. 57(1), 178–203.

[2] Arruda, E.M., Boyce, M.C., 1993. A three-dimensional constitutive model for the large stretch behavior of rubber elastic materials. J. Mech. Phys. Solids. 41(2), 389–412.

[3] Bažant, P., Oh, B.H., 1986. Efficient numerical integration on the surface of a sphere. ZAMM-Z. Angew. Math. Comput. Mech. 66(1), 37–49.

[4] Billiar, K.L., Sacks, M.S., 1997. A method to quantify the fiber kinematics of planar tissues under biaxial stretch. J. Biomech. 30(7), 753–756.

[5] Bingham, C., 1974. An antipodally symmetric distribution on the sphere. Ann. Stat. 2(6), 1201–1225.

[6] Biron, D., Alvarez-Lacalle, E., Tlusty, T., Moses, E., 2005. Molecular model of the contractile ring. Phys. Rev. Lett. 95(9), 98102.

[7] Boyce, M.C., Arruda, E.M., 2000. Constitutive Models of Rubber Elasticity: A Review. Rubber Chem. Technol. 73(3), 504–523.

[8] Bozec, L., Horton, M., 2005. Topography and mechanical properties of single molecules of type I collagen using atomic force microscopy. Biophys. J. 88(6), 4223–4231.

[9] Buehler, M.J., Wong, S.Y., 2007. Entropic elasticity controls nanomechanics of single tropocollagen molecules RID C-4580-2008. Biophys. J. 93(1), 37–43.

[10] Bustamante, C., Bryant, Z., Smith, S.B., 2003. Ten years of tension: single-molecule DNA mechanics. Nature. 421(6921), 423–427.

[11] Butcher, D.T., Alliston, T., Weaver, V.M, 2009. A tense situation: forcing tumour progression. Nat. Rev. Cancer. 9(2), 108–122.

[12] Cacho, F., Elbischger, P.J., Rodriguez, J.F., Doblare, M., Holzapfel, G.A., 2007. A constitutive model for fibrous tissues considering collagen fiber crimp. Int. J. Nonlinear Mech. 42(2), 391–402.

[13] Chakraborty, N., Wang, M., Solocinski, J., Kim, W., Argento, A., 2016. Imaging of scleral collagen deformation using combined confocal raman microspectroscopy and polarized light microscopy techniques. PLoS One. 11(11), e0165520.

[14] Chandran, P.L., Barocas, V.H., 2005. Affine versus non-affine fibril kinematics in collagen networks: Theoretical studies of network behavior. J. Biomech. Eng. 128(2), 259–270.

[15] Chuong, C.J., Fung, Y.C., 1984. Compressibility and constitutive equation of arterial wall in radial compression experiments. J. Biomech. 17(1):35–40.

[16] Dobrin, P.B., 1978. Mechanical properties of arteries. Physiol. Rev. 58(2), 397–460.

[17] Elosegui-Artola, A., Oria, R., Chen, Y., Kosmalska, A., Perez-Gonzalez, C., Castro, N., Zhu, C., Trepat, X., Roca-Cusachs, P., 2016. Mechanical regulation of a molecular clutch defines force transmission and transduction in response to matrix rigidity. Nat. Cell Biol. 18, 540–548.

[18] Eppell, S.J., Smith, B.N., Kahn, H., Ballarini, R., 2006. Nano measurements with micro-devices: mechanical properties of hydrated collagen fibrils. J. R. Soc. Interface. 3(6), 117–121.

[19] Erdmann, T., Schwarz, U.S., 2004. Stability of Adhesion Clusters under Constant Force. Phys. Rev. Lett. 92(10), 108102.

[20] Flory, P.J., 1961. Thermodynamic relations for high elastic materials. T. Faraday Soc. 57, 829–838.

[21] Fratzl, P., 2008. Collagen: Structure and Mechanics. Springer, New York.

[22] Fung, Y.C., Fronek, K., Patitucci, P., 1979. Pseudoelasticity of arteries and the choice of its mathematical expression. Am. J. Physiol Hear. Circ. Physiol. 237(5), H620–631.

[23] Garcia, A., Peña, E., Laborda, A., Lostale, F., De Gregorio, M.A., Doblare, M., Martinez, M.A., 2011. Experimental study and constitutive modelling of the passive mechanical properties of the porcine carotid artery and its relation to histological analysis: Implications in animal cardiovascular device trials. Med. Eng. Phys. 33(6), 665–676.

[24] Geiger, B., Spatz, J.P., Bershadsky, A.D., 2009. Environmental sensing through focal adhesions. Nat. Rev. Mol. Cell Biol. 10(1), 21–33.

[25] Griffith, L.G., 2002. Tissue engineering–Current challenges and expanding opportunities. Science. 295(5557), 1009–1014.

[26] Hench, L.L., Polak, J.M., 2002. Third-generation biomedical materials. Science. 295(5557), 1014–1017.

[27] Holzapfel, G.A., Gasser, T.C., Ogden, R.W., 2000. A new constitutive framework for arterial wall mechanics and a comparative study of material models. J. Elast. 61(1), 1–48.

[28] Holzapfel, G.A., Sommer, G., Gasser, C.T., Regitnig, P., 2005. Determination of layer-specific mechanical properties of human coronary arteries with nonatherosclerotic intimal thickening and related constitutive modeling. Am. J. Physiol. Circ. Physiol. 289(5), H2048–H2058.

[29] Hunter, P.J., Borg, T.K., 2003. Integration from proteins to organs: the Physiome Project. Nat. Rev. Mol. Cell Biol. 4(3), 237–243.

[30] Huyghe, J.M., Jongeneelen, C.J.M., 2012. 3D non-affine finite strains measured in isolated bovine annulus fibrosus tissue samples. Biomech. Model. Mechanobiol. 11(1), 161–170.

[31] Iskratsch, T., Wolfenson, H., Sheetz, M.P., 2014. Appreciating force and shape?the rise of mechanotransduction in cell biology. Nat. Rev. Mol. Cell Biol. 15(12), 825–33.

[32] Kuhl, E., Garikipati, K., Arruda, E.M., Grosh, K., 2005. Remodeling of biological tissue: Mechanically induced reorientation of a transversely isotropic chain network. J. Mech. Phys. Solids. 53(7), 1552–1573.

[33] Langer, R., Tirrell, D.A., 2004. Designing materials for biology and medicine. Nature. 428(6982), 487–492.

[34] Lutolf, M.P., Hubbell, J.A., 2005. Synthetic biomaterials as instructive extracellular microenvironments for morphogenesis in tissue engineering. Nat. Biotechnol. 23(1), 47–55.

[35] MacKintosh, F.C., Kas, J., Janmey, P.A., 1995. Elasticity of semiflexible biopolymer networks. Phys. Rev. Lett. 75(24), 4425–4429.

[36] Marsden, J.E., Hughes, T.J.R., 1994. Mathematical foundations of elasticity. Dover Publications, New York.

[37] Mauri, A., Hopf, R., Ehret, A.E., Picu, C.R., Mazza, E., 2016. A discrete network model to represent the deformation behavior of human amnion. J. Mech. Behav. Biomed. Mater. 58, 45–56.

[38] Miehe, C., Göktepe, S., Lulei, F., 2004. A micro-macro approach to rubber-like materials–Part I: the non-affine micro-sphere model of rubber elasticity. J. Mech. Phys. Solids. 52(11), 2617–2660.

[39] Mooney, M., 1940. A theory of large elastic deformation. J. Appl. Phys. 11, 582–592.

[40] O'Connell, M.K., Murthy, S., Phan, S., Xu, C., Buchanan, J., Spilker, R., Dalman, R.L., Zarins, C.K., Denk, W., Taylor, C.A., 2008. The three-dimensional micro- and nanostructure of the aortic medial lamellar unit measured using 3D confocal and electron microscopy imaging. Matrix Biol. 27(3), 171–181.

[41] Ogden, R.W., 1977. Inequalities associated with the inversion of elastic stress-deformation relations and their implications. Math. Proc. Cambridge Philos. Soc. 81(2), 313–324.

[42] Ogden, R.W., Saccomandi, G., Sgura, I., 2006. On worm-like chain models within the three-dimensional continuum mechanics framework. Proc. R. Soc. A Math. Phys. Eng. Sci. 462(2067), 749–768.

[43] Palmer, J.S., Boyce, M.C., 2008. Constitutive modeling of the stress ? strain behavior of F-actin filament networks. Acta Biomater. 4, 597–612.

[44] Parsons, J.T., Horwitz, A.R., Schwartz, M.A., 2010. Cell adhesion: integrating cytoskeletal dynamics and cellular tension. Nat. Rev. Mol. Cell Biol. 11(9), 633–643.

[45] Peña, J.A., Martínez, M.A., Peña, E., 2015. Layer-specific residual deformations and uniaxial and biaxial mechanical properties of thoracic porcine aorta. J. Mech. Behav. Biomed. Mater. 50, 55–69.

[46] Perumal, S., Antipova, O., Orgel, J.P.R.O., 2008. Collagen fibril architecture, domain organization, and triple-helical conformation govern its proteolysis. Proc. Natl. Acad. Sci. 105(8), 2824–2829.

[47] Reynolds, D.J., Blume, J.A., 1993. Incompressibility and materials with complementary strain-energy density. J. Elast. 33(1), 89–105.

[48] Rezakhaniha, R., Agianniotis, A., Schrauwen, J.T.C., Griffa, A., Sage, D., Bouten, C.V.C., Van De Vosse, F.N., Unser, M., Stergiopulos, N., 2012. Experimental investigation of collagen waviness and orientation in the arterial adventitia using confocal laser scanning microscopy. Biomech. Model. Mechanobiol. 11(3-4), 461–473.

[49] Sáez, P., García, A., Peña, E., Gasser, T.C., Martínez, M.A., 2016. Microstructural quantification of collagen fiber orientations and its integration in constitutive modeling of the porcine carotid artery. Acta Biomater. 33, 183–193.

[50] Sakalihasan, N., Limet, R., Defawe, O.D., 2005. Abdominal aortic aneurysm. Lancet. 365(9470), 1577–1589.

[51] Salbreux, G., Prost, J., Joanny, J.F., 2009. Hydrodynamics of cellular cortical flows and the formation of contractile rings. Phys. Rev. Lett. 103(5), 58102.

[52] Shen, Z.L., Dodge, M.R., Kahn, H., Ballarini, R., Eppell, S.J., 2008. Stress-strain experiments on individual collagen fibrils. Biophys. J. 95(8), 3956–3963.

[53] Tang, Y., Ballarini, R., Buehler, M.J., Eppell, S.J., 2010. Deformation micromechanisms of collagen fibrils under uniaxial tension. J. R. Soc. Interface. 7(46), 839–850.

[54] Treloar, L.R.G., Riding, G., Gee, G., 1979. A non-Gaussian theory for rubber in biaxial strain. I. mechanical properties. Proc. R. Soc. London. A. Math. Phys. Sci. 369(1737), 261–280.

[55] Wu, P.D., Van Der Giessen, E., 1993. On improved network models for rubber elasticity and their applications to orientation hardening in glassy polymers. J. Mech. Phys. Solids. 41(3), 427–456.

[56] Yao, M., Goult, B.T., Chen, H., Cong, P., Sheetz, M.P., Yan, J., 2014. Mechanical activation of vinculin binding to talin locks talin in an unfolded conformation. Sci. Rep. 4, 4610.

[57] Zulliger, M.A., Stergiopulos, N., 2007. Structural strain energy function applied to the ageing of the human aorta. J. Biomech. 40(14), 3061–3069.